JOURNAL OF VIROLOGY, May 2005, p. 5315–5325 Vol. 79, No. 9
0022-538X/05/$08.00+0 doi:10.1128/JVI.79.9.5315–5325.2005

Array Analysis of Simian Varicella Virus Gene Transcription in Productively Infected Cells in Tissue Culture

Steven B. Deitch,[1] Donald H. Gilden,[1,2] Mary Wellish,[1] John Smith,[1] Randall J. Cohrs,[1]* and Ravi Mahalingam[1]

Departments of Neurology[1] and Microbiology,[2] University of Colorado Health Sciences Center, Denver, Colorado 80262

Received 11 November 2004/Accepted 21 December 2004

Simian varicella virus (SVV) is a neurotropic alphaherpesvirus of monkeys that is a model for varicella pathogenesis and latency. Like human varicella-zoster virus (VZV), SVV causes chicken pox (varicella), becomes latent in ganglia along the entire neuraxis, and reactivates to produce shingles (zoster). We developed macroarrays to determine the extent of viral transcription from all 70 predicted SVV open reading frames (ORFs) in infected cells in tissue culture. Cloned fragments (200 to 400 bp) from the 5′ and 3′ ends of each ORF were PCR amplified, quantitated, spotted onto nylon membranes, and fixed by UV cross-linking. Using a cDNA probe prepared from poly(A)$^+$ RNA extracted from SVV-infected Vero cells at the height of the cytopathic effect (3 days after infection) and chemiluminescence for detection, transcripts corresponding to all SVV ORFs were identified. The abundance of each SVV transcript was compared with that previously demonstrated for VZV in infected tissue culture cells.

Natural infection of humans with varicella-zoster virus (VZV) or monkeys with simian varicella virus (SVV) causes chicken pox (varicella) in their natural hosts. Both viruses spontaneously reactivate years later to produce zoster (shingles). Like VZV, SVV becomes latent in cranial nerve and dorsal root ganglia along the entire neuraxis exclusively in ganglionic neurons (5). The mechanisms of varicella reactivation are not known, although in humans the incidence of zoster correlates with a decline in cell-mediated immunity to VZV during aging and immunosuppression. The cascade of events leading to varicella reactivation cannot be determined in living humans, but it is possible to study ganglia from latently infected monkeys.

Transcriptional analysis applied to ganglia will provide valuable information about SVV gene expression during latency but must first be standardized and quantified in productively infected cells. In tissue culture, SVV and VZV are highly cell associated and do not grow to high titers, and synchronous infection is not possible. Nevertheless, even with unsynchronized infection, a uniform cytopathic effect can readily be demonstrated 72 h after cocultivation of uninfected cells with VZV-infected cells in tissue culture. Our earlier studies which used macroarrays to study VZV gene expression in tissue culture (3) revealed that the optimal time for analysis was at the height of the cytopathic effect (3 days after infection). Thus, we focused our efforts on this single time point and conducted triplicate independent analyses with SVV. SVV macroarrays were constructed, and chemiluminescence was used to detect and quantitate viral transcription from every SVV open reading frame (ORF) in SVV-infected cells in tissue culture.

* Corresponding author. Mailing address: Department of Neurology, Mail Stop B182, 4200 E. 9th Avenue, Denver, CO 80262. Phone: (303) 315-8745. Fax: (303) 315-8720. E-mail: randall.cohrs@uchsc.edu.

MATERIALS AND METHODS

Virus and cells. SVV was propagated by cocultivation of infected and uninfected Vero (African green monkey kidney) cells. SVV-infected cells were scraped, washed, and centrifuged at 1,000 × *g* for 5 min. Cell pellets were immediately frozen in liquid nitrogen and stored at −80°C.

DNA extraction and labeling. SVV nucleocapsids were prepared and DNA was extracted as described previously (1). Virus DNA was digested with restriction enzymes BamHI, BglII, EcoRI, and NcoI. The integrity of SVV DNA was determined by agarose gel electrophoresis. Restriction enzyme-digested SVV DNA (1 μg in 16 μl of double-distilled water) was labeled with digoxigenin using the DIG High Prime DNA labeling and detection starter kit II (Roche Applied Science, Mannheim, Germany).

RNA extraction and PCR. Total RNA was extracted from SVV-infected cells using the RNeasy Midi kit (QIAGEN, Valencia, Calif.). Poly(A)$^+$ SVV mRNA was purified using a mRNA purification kit (Amersham Biosciences, Buckinghamshire, England), treated with 1 U/μg of RQ1 RNase-free DNase (Promega, Madison, Wis.) at 37°C for 30 min, and determined to be DNA free by PCR. All PCRs were performed as described previously (6).

Reverse transcription and cDNA labeling. Poly(A)$^+$ SVV mRNA (2 μg) was mixed with 2 μg of oligo(dT) and 0.3 μg of random primers (Invitrogen, Carlsbad, Calif.), and the mixture (39.6 μl) was heated to 65°C for 5 min. The reaction temperature was decreased to 43°C over 10 min, after which 12 μl of 5× avian myeloblastosis virus buffer (Promega) and 1.4 μl of avian myeloblastosis virus reverse transcriptase (high concentration) (600 U) (Promega), 6 μl of PCR nucleotide mix (Roche Applied Science), and 1 μl of 10-mg/ml bovine serum albumin were added. After incubation at 43°C for 130 min, the mixture was heated to 95°C for 5 min. Four tubes containing 2 μg each of SVV mRNA in 60 μl were reverse transcribed to yield a total of 8 μg of SVV cDNA/RNA hybrid. The SVV cDNA/RNA hybrid was treated with 1 μl each of RNase H (1.5 U/μl) (Promega) and RNase-ONE RNase (10 U/μl) (Promega) at 65°C for 30 min to digest the RNA strand, extracted with phenol-chloroform, and alcohol precipitated. Single-stranded SVV cDNA was labeled with digoxigenin using the DIG High Prime DNA labeling and detection starter kit II (Roche). Unincorporated nucleotides were removed by phenol and chloroform extraction and alcohol precipitation.

Cloning of SVV DNA fragments. SVV DNA fragments (200 to 600 bp) from the 5′ and 3′ ends of each ORF were PCR amplified with forward primers (5′-TTTTCCTTTAGCGGCCGC-SVV DNA-3′ [NotI]) and reverse primers (5′-AGGTTCAATTGGAGCTC-SVV DNA-3′ [SstI]). A 284-bp DNA fragment was also amplified from pGEM3zf$^-$ using forward primers (5′-TTTTCCTTTA GCGGCCGCGGCGCTTTCTCATAGCTCAC-3′ [NotI]) and reverse primers (5′-AGGTTCAATTGGAGCTCCGTCTCGCGTCTATGGTTT-3′ [SstI]). Table 1 lists the primer sequences and their location on the SVV genome (4) of

TABLE 1. SVV oligonucleotide primers used in macroarray

ORF (orientation)	5′ location[a]	Sequence[b]	3′ location[c]	Size[d]	GC%[e]
A-1F[f]	1029	TGCAATATCTTCCGTGATG	1048	204	47.10
A-1R[g]	1232	GCGGCAAAGTTTTAATGACA	1213		
A-2F	1570	TCGGTAAACACCCTCCACA	1588	177	42.90
A-2R	1746	ACGAGTCCACTGCACAACAC	1765		
BF	2396	CCCATCACTTACAACGCAGA	2415	187	44.90
BR	2582	GGGACACAATAACGCACACA	2575		
1F	2733	AGCGCCTATTACTGGGACTT	2752	192	38.00
1R	2924	CCGTGTTCCCAACAGAAACT	2904		
3F	3590	AATGGGAATTCGGATGGTTT	3609	202	42.60
3R	3791	TGGCACCATTTACTCAAGCA	3772		
4-1F	4269	ACACCGGCCTTACAAGATCC	4288	202	40.60
4-1R	4470	AGGCGAGGAGTTATCAACCA	4448		
4-2F	5269	TCTCAAAATTAGGCTGCGTG	5288	205	45.90
4-2R	5473	TCGATGCACCTATCACCAGA	5454		
5-1F	5663	GGCTTACTTGGACTCGTTG	5681	192	41.10
5-1R	5854	TTCGGAGCAAGTCGAACAAT	5835		
5-2F	6527	CCGGAGCCGTAGCATATACA	6546	124	35.00
5-2R	6650	GCGCTGGGAATTAAAACAGA	6631		
6-1F	6697	ACCGCGTGTTCCATTAGGTAA	6717	164	38.40
6-1R	6860	CACATCGAGGAGGAAGAACG	6841		
6-2F	9449	TCTGCGTGTATGGCAAATGT	9468	408	38.70
6-2R	9856	AAGCTGTGCCGTTTCGTACT	9837		
7F	10025	CGCCTACAGGAAGCATTAG	10043	419	42.50
7R	10443	AGCATGGCATTTACACCACA	10424		
8-1F	11067	AACACTTTGGTTGCGGTGTT	11086	279	35.10
8-1R	11345	TATGATGTGTGTGCCCCATT	11326		
8-2F	11675	TGTACCCGGAATCAATCACA	11694	282	43.30
8-2R	11956	TTTTGCTGGATGTTGGAATG	11937		
9AF	12050	GCTCTTTGGAATTGTTCATG	12069	230	43.00
9AR	12279	GGATCGAGTAAATAACCGGAAA	12259	230	
9-1F	12512	TGTACCACGAAGAAGCGTTG	12531	292	41.40
9-1R	12803	TATCATGCGAGGTTGTGCAT	12784		
9-2F	12926	TCCAACACCGGCATATAACA	12945	282	46.50
9-2R	13207	GGCTCATCATCCGTGTCTTT	13188		
10-1F	13641	GGAACACAACGCAGGTTCAT	13660	310	37.40
10-1R	13950	CGGTAGCGAAGGAAGATCAC	13931		
10-2F	14417	ATTATCGCCGCAGACAACTT	14436	306	43.80
10-2R	14722	TCTGTGGAGGATCACCAGGT	14703		
11-1F	15094	ATTAGCATCCCCAGCAACAG	15113	262	43.50
11-1R	15355	GGACGGGAACAGGTTTCTCT	15336		
11-2F	16714	ATTACTGCCACCAGCCCTTT	16733	266	41.40
11-2R	16979	CAATCAATCCCAACAATTTCA	16959		
12-1F	17188	CAAACCGGAAAAATGTAATGG	17208	272	41.50
12-1R	17459	TTGTCCGTTGACATACACGA	17478		
12-2F	18774	CGCAGGTTAAAGCAGCCT	18791	269	43.50
12-2R	19042	TGCCAGAGCTATCAAGCAAA	19061		
13-1F	19329	AACAGATCGAACCGGAACTG	19348	275	37.80
13-1R	19603	TCAGCTCCAAAATGTCTCCA	19622		
13-2F	19729	GCCTGGAACGCTAAAGATGT	19748	302	39.40
13-2R	20030	ATGCGAAGAGTTGGGAATTG	20011		

Continued on facing page

TABLE 1—*Continued*

ORF (orientation)	5′ location[a]	Sequence[b]	3′ location[c]	Size[d]	GC%[e]
14-1F	20317	ACGTTGATGCTGATGAGGAC	20336	236	41.10
14-1R	20552	TGTTTAGCCAGTTGTGTTCCT	20572		
14-2F	21451	GGGTTGTTTGGGTGTGAAA	21469	311	58.50
14-2R	21761	AACGCCGCAGTTACATCAA	21743		
15-1F	22074	AAACCACACATGCTCCCATT	22093	313	31.00
15-1R	22386	GCCGGTGTTTTGGTTATGTT	22367		
15-2F	22932	ACTGTTGCCCTGAAGTCCA	22950	261	31.00
15-2R	23192	CGGCAAAATGTGTTCCTTGT	23173		
16-1F	23429	ATCTGCTCCGATTCCACATT	23448	305	39.30
16-1R	23733	ACAGCGGTTTTCGTTCTACC	23714		
16-2F	24155	GGATACGCATTTCGGTGAA	24173	290	40.30
16-2R	24444	CAGAAGTTGGAAGGGCTACG	24425		
17-1F	24775	CATGGGGCTCTTTGGACTT	24793	293	38.90
17-1R	25067	TTGCTCCTCGTGCTAAAGGT	25048		
17-2F	25763	GATTTACAACCCGGTGACCTT	25783	334	40.10
17-2R	26096	GGAGTGGGGGAGCAAGTAA	26078		
18-1F	26238	TGGTGTGTTTTTCCGCTGT	26256	291	38.10
18-1R	26528	TCCATACAAGTGCTTCTTGCTG	26508		
18-2F	26757	GACGTTCAAAAATATCGCCTTC	26777	319	32.60
18-2R	27075	CTGGAATGCCCGGATATAAA	27056		
19-1F	27166	CCGCTATTTGTAGCCTTTCG	27183	248	38.30
19-1R	27413	TTAAACGCTCGTCATCCTCT	27394		
19-2F	29165	AACACTGAATCGCTCTCCTCA	29185	301	39.20
19-2R	29465	AGCTACAGCCCGTCAAACA	29447		
20-1F	29749	ACGTTCCATTTTTCGTGCA	29767	301	44.20
20-1R	30049	GTTTTTATTGGGCCGCATTC	30030		
20-2F	30711	CATCTGGACGACATAAATCTGTT	30731	303	32.70
20-2R	31013	CGAACGTAATGTTAATGGGAGA	30992		
21-1F	31272	CCCAACCGTGGATATTATGG	31291	306	36.90
21-1R	31577	TTTTGTGTGCAATGCGATTC	31558		
21-2F	34044	CGACAGAACATCTACCCCAGA	34064	269	37.20
21-2R	34312	TCATAAGCCATCTTTGTTCGATT	34290		
22-1F	34664	CCCAACCGTGGATATTATGG	34684	287	37.30
22-1R	34950	TTTTGTGTGCAATGCGATTC	34290		
22-2F	42223	ACATAACAAGGCAATCTCACG	42243	277	48.40
22-2R	42499	GGTAACGTCTGCGTTCAACA	42480		
23-1F	43184	TTACACCCGCCGACTACTTC	43203	299	49.80
23-1R	43482	AACAACCACCCCCTTCAAA	43464		
23-2F	43588	TTGGTCGAAGCCATGTCA	43605	261	44.40
23-2R	43848	GAGCGCATTTTGATCCATCT	43829		
24-1F	43973	CCCCAAAGTAACGGCAGA	43990	275	38.20
24-1R	44247	CAGAAGATCCAACCCGTACA	44228		
24-2F	44252	CATGAAACGAAAAGCAAGTTGT	44273	284	38.00
24-2R	44535	ATTGGGCAGAATGCGTATGT	44516		
25F	45020	GGACGAAAAACGATCCGTAA	45039	306	37.30
25R	45325	GAAAACGCATCTGACAACCA	45306		
26-1F	45306	TGGTTGTCAGATGCGTTTTC	45325	371	36.40
26-1R	45676	TCAAACCAAACCTCCGTTT	45558		
26-2F	46667	TTGCGATCCTTTTTGTGCT	46685	283	42.00
26-2R	46949	GGTATGTTCGAGGGAGACCA	46930		

Continued on following page

TABLE 1—*Continued*

ORF (orientation)	5′ location[a]	Sequence[b]	3′ location[c]	Size[d]	GC%[e]
27-1F	46927	CACTGGTCTCCCTCGAACA	46945	257	40.90
27-1R	47183	TCAAATGGAAGCGTTACAGG	47164		
27-2F	47601	CATTTTAGCCGCATGTAGGG	47620	222	36.90
27-2R	47822	CGAGGAGGAACAAAGTCGTC	47803		
28-1F	47758	GATGGGGAATTGCTTCTTGA	47777	313	35.80
28-1R	48070	GTGTATGCTGCTGGACATGG	48051		
28-2F	51039	TCATATTCACGTCCATCGTAGT	51060	208	34.60
28-2R	51246	TGGCTAACAGAACAGATTTTTG	51267		
29-1F	51477	AACTGGCCCTTTGGGTTAC	51504	267	39.30
29-1R	51743	CCACCGTGAAATACAAATGC	51724		
29-2F	54792	TTCTGATGCCGTTTTAGAAGC	54812	243	38.70
29-2R	55034	ACCATATCCATTGTAAGGCTCA	55013		
30-1F	55184	CCTTTCAAATGGAACTCCTACG	55204	201	36.30
30-1R	55384	GCCTCTGCTTCGTATTGAAGA	55364		
30-2F	57135	TTTCATTGTGGAGAGGTTGCT	57155	250	38.80
30-2R	57384	GAACAAGCCGCTGAATTAGA	57365		
31-1F	57270	CCCCTGATTGCAGTATTACACA	57291	310	38.40
31-1R	57579	GATTCGTGGAGAGCCTTTCT	57560		
31-2F	59732	GCTGATGGTGTCGATCCTTT	59751	249	39.00
31-2R	59980	ACGTGATTTACCCCGGTTCT	59961		
32F	60192	CTACAACCGCTGCATTGACA	60211	305	45.90
32R	60496	CCAGTCTTCTTCTGGCGTGT	60477		
33-1F	60647	TACATTCGGCCACACATCA	60665	296	44.60
33-1R	60942	CGGCAGGAAATAAGTGAGTTG	60922		
33-2F	62098	CACGTAAAGCAGACGCTCAG	62117	287	41.80
33-2R	62384	TAGCGGGTTATTTGGCGTT	62366		
33.5F	61209	TACCCCTATCAGCAGCCAAC	61228	299	42.10
33.5R	61507	GGCCGCTAGTGTTACAAACG	61498		
34-1F	62445	ACGCCACAGAGGTAAACTGG	62464	255	38.00
34-1R	62699	TTATGCGGCTTATCGCTCTT	62680		
34-2F	63921	GCGGCTTTAATCTACGCTCA	63940	167	43.70
34-2R	64087	TCCTTCGTACTGGACGGAAC	64068		
35-1F	64279	AAGCCCTCCGAAGTACGTTT	64298	226	39.80
35-1R	64504	CTTACGTGGTAATGCGGTTG	64485		
35-2F	64690	AGATGTAAACCGACACGATTTT	64711	298	30.20
35-2R	64987	TCTCCAGAAGCGTTTTCGAC	64968		
36-1F	65036	TGCAGAGATCCGGTTTGTATT	65056	226	44.20
36-1R	65261	GTGCGTCGTTATCGGAGATT	65242		
36-2F	65759	GAAAACCCAGTAATTGAAAACACA	65782	261	38.30
36-2R	66019	CGAATCGGACATTTCTTGTAAA	65998		
37-1F	66243	ACGCTACACAGAAACCATG	66261	309	38.50
37-1R	66551	GCGAGGCGGAGATTTAAGTT	66532		
37-2F	68528	CGCTTTTAACCCAGACGTTC	68547	230	40.40
37-2R	68757	CCAAAGGGACAGCGGTATATT	68737		
38-1F	68827	GTGTGCGGGGATTTAATGT	68845	202	36.60
38-1R	69028	TTATATGCCGGGGAAAGTTG	69009		
38-2F	70098	CCGCATAAATCACGTTCGTT	70117	240	43.30
38-2R	70337	TTTTATTTGCGGGGGTTGT	70319		
39-1F	70719	GAAAAACGAAGAGTCGGGTTC	70739	283	32.90
39-1R	71001	TGCAAGACGAAAGTAGTGGA	70982		

Continued on facing page

TABLE 1—*Continued*

ORF (orientation)	5′ location[a]	Sequence[b]	3′ location[c]	Size[d]	GC%[e]
39-2F	71047	CCACTATCCACATCACAGCAG	71067	300	35.70
39-2R	71346	CCTCATTAAAGCCCGTACCC	71327		
40-1F	71591	AAACCGCCTTTCCAGCTT	71608	272	38.60
40-1R	71862	CACCATCACGAACATATCC	71844		
40-2F	75479	AGAATCTCGTGCGGTTTGTT	75498	242	44.20
40-2R	75720	CAGACAGACAACCCCGTATG	75701		
41-1F	75870	GCCCAACGAAACGTCTAAC	75888	242	43.00
41-1R	76111	AAAGTCCAGGGGCGTTAAA	76093		
41-2F	76402	GCCAACGCCGTAAATATGTC	76421	300	40.70
41-2R	76701	AATTGCCTTTGTTCCCAATG	76682		
42/45-1F	76854	AGATGTTTCCATCCCTCCAA	76873	306	37.60
42/45-1R	77159	CCAGGGAGTCAAGTGGCA	77142		
43-1F	78085	AACGATACAACAAGAGGCATGA	78106	269	39.00
43-1R	78353	TGGGTACGGATAGAAACAACC	78373		
43-2F	79693	CCGTGTTGGTTGGGAAATAG	79712	335	39.40
43-2R	80027	GGACCAATAAGTGACGTTGGA	80007		
44-1F	80262	TCTGCGCGAATACTAACACC	80281	249	41.60
44-1R	80511	CATGAAAGTGTTTCTGCGGT	80492		
44-2F	80958	CCCAATCACACAGAAAGCTG	80977	297	43.00
44-2R	81255	GAAGAAGCGCACATCCATT	81237		
42/45-2F	82118	TTTTACCCGTTCCATCCTTG	82137	302	38.40
42/45-2R	82419	TGGTAATAAGGTAGGCGAGCA	82399		
46-1F	82543	GCACCACGCAACTTTCAA	82560	272	42.30
46-1R	82814	TTTTCGTATGGTTGTTTGTTCC	82793		
46-2F	82841	AGCGCCAAACTTCGTAGAAC	82860	278	46.40
46-2R	83118	TGTTTGTCATCGCGTTTTTC	83099		
47-1F	83026	CTCCACCAACCCAAAACACT	83045	286	39.50
47-1R	83311	CCTTGATAACTGCGATATTCTAAACA	83286		
47-2F	84193	GGACACACTGGCATATCGTG	84212	301	43.20
47-2R	84493	CCAGCTTGGATTTTGCCA	84476		
48-1F	84475	ATGGCAAAATCCAAGCTG	84492	286	34.30
48-1R	84760	TGAATAGTTCTTTGCAGGCTGA	84739		
48-2F	85686	CAATCCACGCCACCTAAACT	85705	286	40.60
48-2R	85971	GCGTGCCTCGTTTTCAATT	85953		
49F	86005	TGGGTCAAACAACATCTACTGG	86026	150	43.30
49R	86154	GATTACCAGCCTCGTTGGTC	86135		
50-1F	86395	TTATCACGCGGAAGATTTG	86413	300	38.00
50-1R	86694	AGCTGCTCATGCGTATATGG	86675		
50-2F	87348	TGCCCCATATCCTTTATTTCC	87368	308	42.20
50-2R	87655	TGTTCGTGTCTTCGACGTTT	87636		
51-1F	87692	GCGTTATATGGAGCCGATTT	87711	220	45.50
51-1R	87911	AAACTTCGTCGGCAAGACAC	87930		
51-2F	89747	CGTTTAGTGTGGGAACAGCTT	89767	293	33.40
51-2R	90039	AACATTGGCAACTGGGTGTT	90015		
52-1F	90271	GGTTGTATTTGTGCGGCTAGT	90291	264	44.30
52-1R	90534	ACGCCACATATCGCAGTTG	90552		
52-2F	92204	GTACACCCGACGGAGCTTT	92222	260	40.40
52-2R	92463	TGGAGTTTCAACATCAAAGTCA	92484		
53-1F	92684	CGCTTCTTAGAGGTGCGTTC	92703	233	40.30
53-1R	92916	TACGTTAATGCGGCTTGTTG	92896		

Continued on following page

TABLE 1—*Continued*

ORF (orientation)	5′ location[a]	Sequence[b]	3′ location[c]	Size[d]	GC%[e]
53-2F	93204	CGGCTGTTGTTGACATTGTT	93223	292	38.70
53-2R	93495	CGTCCAAATACCAAGCGTTC	93476		
54-1F	93432	TTCCGCTCGCACTAAGAGA	93450	318	36.80
54-1R	93749	TGGAGGCGTATTTGACACAA	93730		
54-2F	95295	TCAATAACACGGTTGCCTGA	95314	288	40.60
54-2R	95582	GCAAAAGTACCGATGTGCAA	95563		
55-1F	95749	CGAACTTGCCTCGGAAACT	95767	226	42.50
55-1R	95974	GTTTTGTGCCGCAATTCTG	95956		
55-2F	97968	ACGACGCAGAGCTTACAATG	97987	265	41.90
55-2R	98232	GGATCTCGTAGCGCCTCTAA	98213		
56-1F	98334	TTGGTGTTCGCCTCTAACAA	98353	224	37.90
56-1R	98557	AATCTGTCATCCCATCCAATG	98537		
56-2F	98627	TCGTTCCCTTTGAAAATTGG	98646	194	37.60
56-2R	98820	TTGTCGTAAACGTGGCTCCT	98801		
57F	98955	GCGTGCGCTGTGTTGTTC	98972	154	44.80
57R	99108	GAGCGAAACAATGTGCGTTT	99089		
58-1F	99137	TGTTCCAGATGTTAGCAGTTC	99158	250	40.80
58-1R	99386	AATCAAAAAGCCGGAAGCT	99368		
58A-2F	99490	ATTGTCTTCTGCCCGGTTC	99508	219	38.40
58A-2R	99708	TACAGTGGGGTTGGGGAGAA	99689		
59-1F	99778	ATGGGTTCTCCTCGTTTCAA	99797	311	41.80
59-1R	100088	GATAATTGGGCTCGACAAGG	100069		
59-2F	100331	CCCGCTGTCTGTATTGTTCA	100350	296	38.90
59-2R	100626	TGTGTTTGAGCGAAAAAGGA	100607		
60-1F	100611	TTTTCGCTCAAACACAGAC	100629	212	43.90
60-1R	100822	CACATGGCGTATTGGGTAAA	100803		
60-2F	100907	TACCGAAGGCGCTGAGTATT	100926	164	29.30
60-2R	101070	TGGAAGGACATAGGTTTGTTTT	101091		
61-1F	102303	AATGCGAGCAATACCCTGTT	102322	275	48.40
61-1R	102577	GTAGACGCCCAGGTAGACCA	102558		
61-2F	103502	TCTGTAATGGTGCATCTTCGTT	103523	203	45.80
61-2R	103704	CTCCGGTCTCGGTAAAACCT	103685		
62-1F	104647	GACGAGGACATCCACTCCAT	104666	297	72.10
62-1R	104943	CGAGGATGACGGTGAAGG	104926		
62-2F	108129	GGCCAAATCCACCAAAGAA	108148	283	50.90
62-2R	108411	TCCCAGTGCATTAGAGCTGA	108392		
63-1F	109853	CCCCGAGATGAAATGAC	109869	278	51.80
63-1R	110130	CGGCCCATTAAGTAAAAATCA	110110		
63-2F	110331	ATGACGACCAATCAACCACA	110350	249	48.20
63-2R	110579	TATGCTCTACCGAGGCGTTG	110560		
64-1F	110853	GGATTTATACAGGGCCGAAC	110872	271	57.60
64-1R	111123	CACGGCAGGGAAGGATATT	111105		
64-2F	111131	CAACACTGGCGGTTCTCC	111148	258	51.60
64-2R	111388	CGTGTTTTATGTTGCGGTCT	111369		
65F	111723	AAACCAAAAATGTAACACGCTTT	111745	210	38.10
65R	111932	ATAGTGAGGCCGTAGCGTTG	111913		
66-1F	112442	TACGATATGCTTGCGGATG	112460	251	45.00
66-1R	112692	CGTATGATTACCGGGTGGTT	112673		
66-2F	113169	CTGGAGTTCATCCCAGTGAA	113188	241	43.20
66-2R	113409	GGATATGGGTCCGGTATATCA	113389		

Continued on facing page

TABLE 1—*Continued*

ORF (orientation)	5′ location[a]	Sequence[b]	3′ location[c]	Size[d]	GC%[e]
67-1F	113730	CGCGGCAATTATTTATAGGG	113749	247	38.50
67-1R	113976	ACCAGTGCGAATACGTGGA	113958		
67-2F	114449	CCGCAGATGTATTTATGATTG	114469	241	41.10
67-2R	114689	TGTGGAGGGTTTTCCTCTTG	114670		
68-1F	114977	TCTGCGGAACACTATCATGG	114996	289	37.40
68-1R	115265	TTGTTTCCATCTCCCAATTCTT	115244		
68-2F	116437	CCATCATCGCCCAATGTTAC	116456	262	47.70
68-2R	116698	CGCCTTCGTCTACCTCAACT	116679		

[a] 5′ location of primer.
[b] Sequence of primer.
[c] 3′ location of primer.
[d] Size of amplified fragment (bp).
[e] Molar G+C content of amplified fragment.
[f] Forward primer (F) with the sequence TTTTCCTTTAGCGGCCGC containing NotI (GCGGCCGC) attached at the 5′ end of each of the SVV sequences.
[g] Reverse primer (R) with the sequence AGGTTCAATTGGAGCTC containing SstI (GAGCTC) attached at the 3′ end of each of the SVV sequences.

oligonucleotide primers for all SVV ORFs, as well as the G+C content of each amplified segment. Computer analysis of DNA sequences was performed using DNAMax (MiraiBio, Inc., Alameda, Calif.). PCR products were digested with NotI and SstI and inserted directionally in the multiple cloning sites of pGEM11zF (Promega). The concentrations of all recombinant plasmids were determined by absorbance at 260 nm and diluted to 30 ng/μl. The cloned SVV or pGEM3zf$^-$-specific inserts were amplified using vector-specific primers (GEMF [5′-CCCAGTCACGACGTTGTAAA-SVV DNA-3′] and GEMR [5′-TCACACAGGAAACAGCTATG-SVV DNA-3′]). The closed segment of pGEM3zf$^-$ and no DNA were used as negative controls. Actin, a positive control for cellular transcription, was amplified as described previously (2).

Array construction. SVV DNA fragments and positive and negative controls were amplified, quantitated, spotted (40 ng/4 μl) onto a 200-cm^2 neutral BioBond nylon membrane (Sigma-Aldrich, St. Louis, Mo.) and fixed by UV cross-linking twice at 125 mJ using the GS gene linker (Bio-Rad, Hercules, Calif.).

Hybridization and detection. The UV-fixed target SVV DNA fragments were prehybridized in a hybridization oven (Boekel Scientific, Feasterville, Pa.) for 3 h at 42°C in 35 ml of Digoxigenin Easy hybridization solution (Roche Applied Science) in glass cylinders (35 by 300 mm) (VWR Scientific Products, Brisbane, Calif.). Digoxigenin-labeled DNA (2 μg) or cDNA (8 μg) was denatured at 95°C for 10 min and quenched on ice for 5 min. The prehybridization solution was replaced with 20 ml of fresh hybridization solution containing probe and hybridized for 48 to 72 h at 42°C. The nylon membrane was washed in 35 ml of 0.1× SSC (1× SSC is 0.15 M NaCl plus 0.015 M sodium citrate) and 0.1% sodium dodecyl sulfate at room temperature (three times for 5 min each and twice for 15 min each) and then in 90 ml of washing buffer (100 mM maleic acid, 150 mM NaCl) for 5 min at room temperature. The membrane was then placed in 30 ml of blocking solution (3 ml of 10× blocking solution [DIG High Prime DNA labeling and detection starter kit II; Roche Applied Science] with 27 ml of maleic acid buffer [0.1 M maleic acid, 0.15 M sodium chloride]) for 2 h at room temperature. The membranes were treated using one of the following two methods. (i) The membranes were incubated in 28 ml of alkaline phosphatase-conjugated antidigoxigenin Fab fragments (2.8 ml of blocking solution, 25.2 ml of maleic acid buffer, 1.4 μl of antidigoxigenin antibodies [1:20,000]; Roche Applied Science) for 1 h at room temperature, washed at room temperature with 140 ml of blocking solution (14 ml of 10× blocking solution with 126 ml of maleic acid buffer) three times for 8 min each time, and washed at room temperature with 140 ml of washing buffer (99.62 mM Tris-HCl, 99.25 mM NaCl, pH 9.5) twice for 8 min. (ii) The membranes were incubated with 40 ml of peroxidase-conjugated antidigoxigenin poly-Fab fragments (4 ml of blocking solution, 36 ml of 100 mM Tris-HCl, pH 7.5, 150 mM NaCl, 120 μl of antidigoxigenin antibodies [1:333]; Roche Applied Science) for 2 h at room temperature and washed by the washing protocol described above. Chemiluminescence detection was performed twice using two different preparations of mRNA with the CDP-Star detection reagent (New England BioLabs, Beverly, Mass.) and once using another independent preparation of mRNA with the ECL Western Blotting Detection Reagents and Analysis System (Amersham Bioscience, Piscataway, N.J.). Hybridization signals were detected using Kodak Biomax Light film. Uninfected Vero cells were treated by identical protocols.

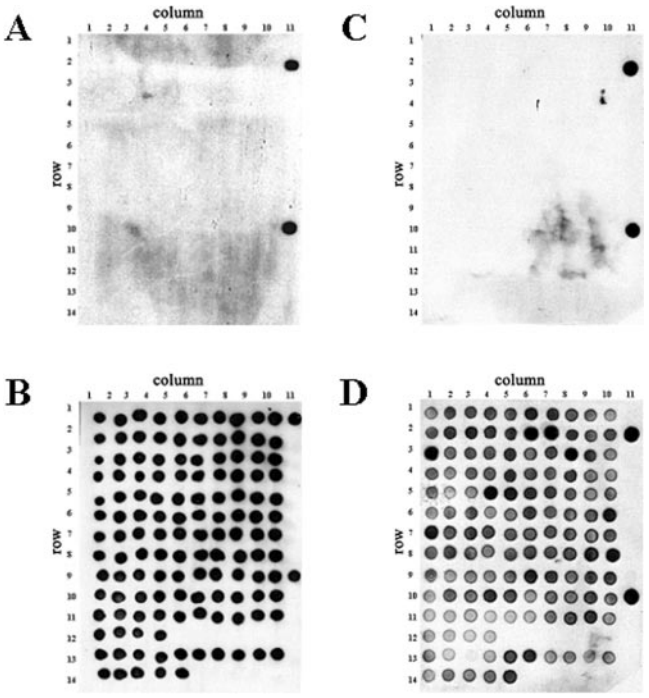

FIG. 1. Specificity of SVV arrays. The arrays contain target DNA fragments from the 5′ and 3′ ends of each of the 70 predicted SVV ORFs. Fragments corresponding to each SVV ORF were quantitated, spotted onto a nylon membrane, and fixed as described in Materials and Methods. Arrays were hybridized to digoxigenin-labeled DNA from uninfected (A) and SVV-infected Vero cells (B) and to digoxigenin-labeled cDNA probes prepared from poly(A)$^+$ RNA extracted from uninfected (C) or SVV-infected Vero cells 3 days after infection (D). Signals were detected using antidigoxigenin antibodies conjugated to horseradish peroxidase and detected by chemiluminescence. Table 2 lists the location (column and row) of the 70 SVV DNA ORF targets. Each array contained two sets of three controls: array B contained actin (column 11, rows 1 and 9), pGEM (column 11, rows 2 and 10), and no DNA (column 11, rows 3 and 11). Arrays A, C, and D contained actin (column 11, rows 2 and 10), pGEM (column 11, rows 1 and 9), and no DNA (column 11, rows 3 and 11).

TABLE 2. Quantitative analysis of SVV gene transcription 3 days after infection

ORF	Region	Location on array[a]		Relative expression[b]	SD[c]	Order[d]
		Row	Column			
A	3′	1	1	50.0	9.8	45
A	5′	1	2	44.9	8.0	48
B	All	1	3	48.1	12.0	50
1	All	1	4	48.9	2.0	27
3	All	1	5	44.7	7.4	43
4	3′	1	6	60.0	1.5	11
4	5′	1	7	60.7	12.8	17
5	3′	1	8	48.3	10.8	37
5	5′	1	9	39.6	5.0	70
6	3′	1	10	36.9	3.9	112
6	5′	2	1	52.1	12.8	77
7	All	2	2	55.6	7.1	34
8	3′	2	3	55.5	5.5	19
8	5′	2	4	64.4	9.8	16
9A	All	2	5	58.9	5.9	25
9	5′	2	6	95.3	26.1	2
9	3′	2	7	100.0	30.9	1
10	5′	2	8	44.4	3.5	38
10	3′	2	9	42.8	7.1	54
11	5′	2	10	48.9	3.7	42
11	3′	3	1	91.1	23.5	4
12	5′	3	2	34.1	8.4	94
12	3′	3	3	39.1	4.1	40
13	5′	3	4	56.7	7.1	22
13	3′	3	5	57.1	2.0	15
14	3′	3	6	48.1	3.8	35
14	5′	3	7	51.5	0.7	30
15	3′	3	8	68.0	1.4	9
15	5′	3	9	46.4	4.6	32
16	3′	3	10	34.7	8.3	98
16	5′	4	1	33.5	6.4	75
17	5′	4	2	28.2	5.5	110
17	3′	4	3	39.2	3.0	55
18	3′	4	4	49.6	2.0	33
18	5′	4	5	50.2	7.7	20
19	3′	4	6	49.5	3.1	39
19	5′	4	7	37.0	5.3	91
20	3′	4	8	50.5	10.2	41
20	5′	4	9	34.4	12.4	102
21	5′	4	10	33.3	12.2	114
21	3′	5	1	39.7	3.7	68
22	5′	5	2	29.8	7.9	106
22	3′	5	3	32.3	3.5	86
23	3′	5	4	94.6	26.2	3
23	5′	5	5	78.0	9.4	5
24	3′	5	6	54.5	3.9	21
24	5′	5	7	57.9	8.8	44
25	All	5	8	33.4	11.0	109
26	5′	5	9	32.1	11.6	115
26	3′	5	10	37.2	15.0	82
27	5′	6	1	40.3	8.3	101
27	3′	6	2	48.5	8.2	58
28	3′	6	3	57.4	7.4	29
28	5′	6	4	31.6	1.5	97
29	5′	6	5	42.0	6.4	78
29	3′	6	6	54.2	4.4	31
30	5′	6	7	37.8	7.1	104
30	3′	6	8	37.8	13.1	107
31	5′	6	9	43.4	6.4	73
31	3′	6	10	62.0	11.1	13
32	All	7	1	94.7	30.5	8
33	3′	7	2	69.2	14.0	47
33	5′	7	3	57.3	5.1	23
33.5	All	7	4	55.6	3.7	28
34	3′	7	5	48.7	10.6	65
34	5′	7	6	42.4	8.3	69
35	3′	7	7	45.0	6.4	90
35	5′	7	8	34.4	12.6	87
36	5′	7	9	35.8	12.8	96
36	3′	7	10	36.2	11.2	81
37	5′	8	1	43.0	4.4	88
37	3′	8	2	71.3	13.2	51
38	3′	8	3	50.6	1.5	67
38	5′	8	4	40.0	2.2	92
39	5′	8	5	49.2	11.7	64
39	3′	8	6	49.2	10.9	49
40	5′	8	7	44.6	6.2	84
40	3′	8	8	44.4	12.2	60
41	5′	8	9	68.5	3.8	36
41	3′	8	10	79.0	14.9	18
42.45	3′	9	1	53.0	9.1	76
42.45	5′	9	2	36.4	3.6	122
43	5′	9	3	44.0	6.3	108
43	3′	9	4	42.2	5.7	85
44	5′	9	5	49.9	11.3	74
44	3′	9	6	64.2	8.6	26
46	5′	9	7	50.1	10.1	52
46	3′	9	8	43.4	4.0	103
47	5′	9	9	46.1	9.1	83
47	3′	9	10	53.3	5.7	61
48	5′	10	1	43.9	12.2	111
48	3′	10	2	67.5	15.0	59
49	All	10	3	70.9	20.1	53
50	3′	10	4	81.8	18.3	12
50	5′	10	5	73.5	13.8	14
51	5′	10	6	41.3	5.6	116
52	3′	10	9	51.5	4.4	56
53	3′	10	10	53.5	10.0	79
53	5′	11	1	43.2	13.8	113
54	3′	11	2	40.1	11.1	126
54	5′	11	3	37.3	6.4	120
55	5′	11	4	32.7	8.5	123
55	3′	11	5	47.1	16.5	117
56	5′	11	6	41.3	11.5	119
56	3′	11	7	46.3	5.9	66
57	All	11	8	67.8	9.6	46
58	3′	11	9	72.4	8.2	24
58	5′	11	10	46.5	8.1	93
59	3′	12	1	59.3	22.4	89
59	5′	12	2	43.0	14.9	125
60	3′	12	3	35.5	11.5	128
60	5′	12	4	36.3	9.9	124
61	3′	13	1	66.8	22.0	72
61	5′	13	2	45.9	19.6	127
62	3′	13	3	28.3	16.8	129
62	5′	13	4	42.1	11.6	121
63	5′	13	5	91.1	32.7	10
63	3′	13	6	93.4	33.2	7
64	5′	13	7	54.0	14.1	80
64	3′	13	8	57.9	12.9	71
65	All	13	9	30.5	6.2	118
66	5′	13	10	42.1	1.8	63
66	3′	14	1	42.8	11.0	105
67	5′	14	2	52.8	17.0	95
67	3′	14	3	51.8	18.6	99
68	5′	14	4	55.4	8.7	57
68	3′	14	5	90.7	28.8	6
Avg array controls						
pGEM		1	11	0.2	0.1	131
Actin		2	11	1.0	0.0	134
No DNA		3	11	0.2	0.1	132

[a] See Fig. 1 for array with column and row designations.
[b] Relative ORF transcription normalized according to the equation in Materials and Methods.
[c] Standard deviation for each ORF.
[d] Order in decreasing magnitude of the relative expression for each array target.

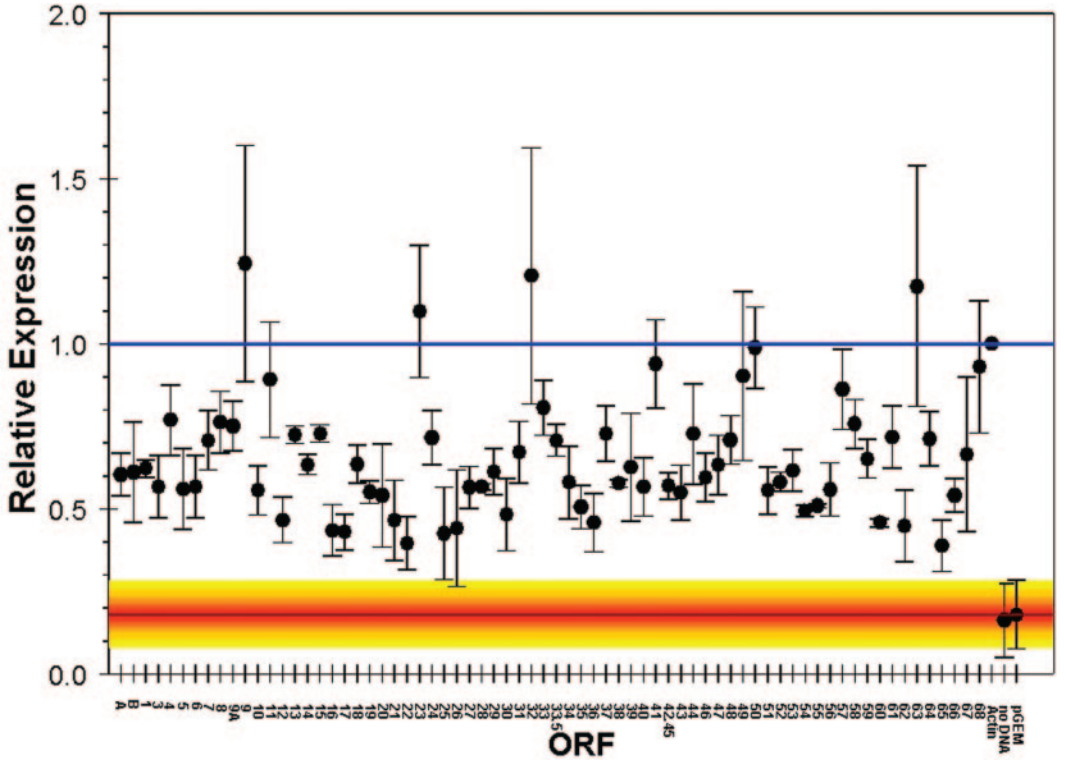

FIG. 2. Transcription of SVV ORFs in SVV-infected Vero cells in culture. The ORF numbers are shown on the *x* axis, and the level of expression relative to actin is shown on the *y* axis. Each data point indicates the average spot intensity for each ORF (average of the 5′ and 3′ ends). Each error bar indicate the standard deviation for each data point. Expression levels of array controls (actin, no DNA, and pGEM) are shown at the lower right.

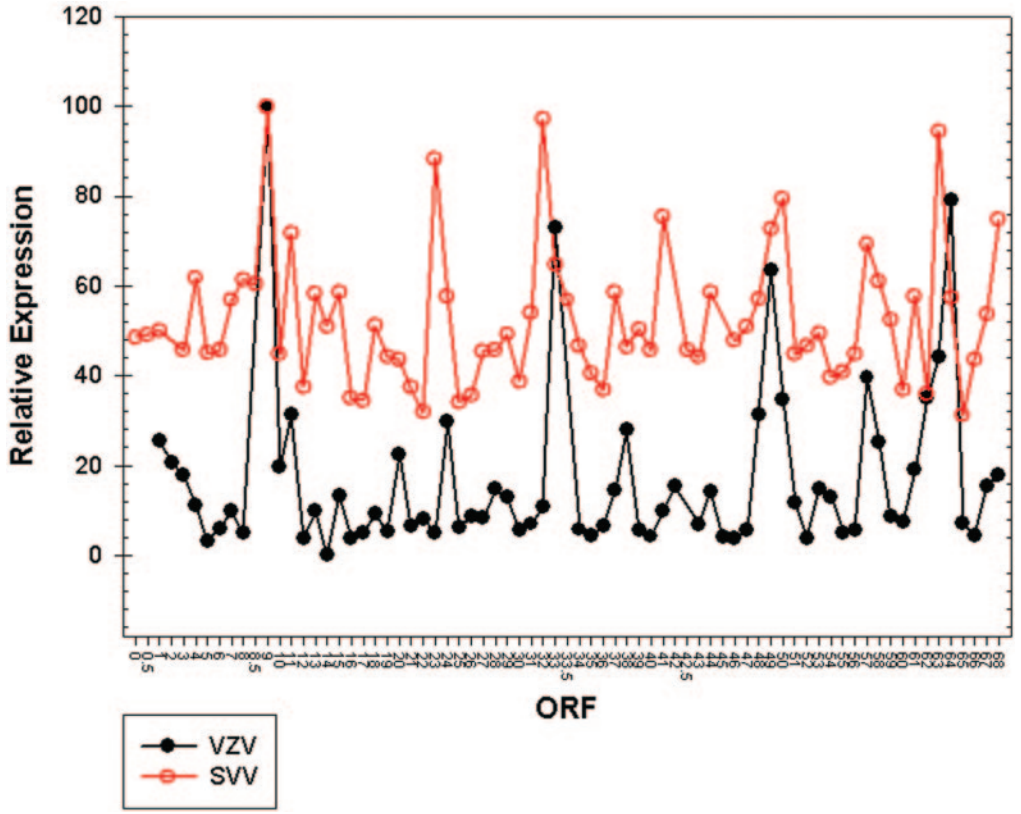

FIG. 3. Comparative transcription of SVV and VZV ORFs in cells 3 days after infection. The graph shows the average spot intensities of all predicted SVV and VZV ORFs. On the *x* axis, ORF 0 is SVV ORF A, ORF 0.5 is SVV ORF B, and ORF 42.5 is SVV ORF 42.45. Note that transcripts corresponding to ORF 9 (encoding the tegument protein) and 63 (an immediate-early gene) are among the five most abundantly expressed genes by both viruses.

TABLE 3. Relative expression of SVV ORFs during lytic infection

ORF	Relative expression	VZV gene function
A	48.61	Truncated homolog of VZV ORF 4
B	49.21	Homolog of VZV ORF S/L
1	50.08	Membrane protein
3	45.74	Virion assembly
4	61.80	Transcriptional activator, IE protein 2[a]
5	44.99	Glycoprotein K
6	45.57	Component of DNA helicase-primase complex
7	56.91	Virion phosphoprotein
8	61.37	Glycoprotein N
9A	60.36	Glycoprotein N
9	100.00	Tegument protein that is a major viral structural component capable of nuclear shuttling and may play a role in virus entry and/or egress
10	44.67	Transcriptional activator, tegument protein
11	71.66	Tegument protein
12	37.49	Tegument protein
13	58.27	Thymidylate synthetase
14	50.99	Glycoprotein C
15	58.54	Membrane protein
16	34.93	Associated with DNA polymerase
17	34.50	Host shutoff virion protein
18	51.10	Ribonucleotide reductase, small subunit
19	44.27	Ribonucleotide reductase, large subunit
20	43.45	Capsid protein
21	37.39	Tegument protein
22	31.82	Tegument protein
23	88.36	Capsid protein
24	57.55	Membrane phosphoprotein
25	34.20	Viral DNA cleavage/packaging
26	35.47	DNA cleavage/packaging
27	45.46	Nuclear phosphoprotein
28	45.56	DNA polymerase
29	49.25	Single-stranded DNA binding protein
30	38.74	Viral DNA cleavage/packaging
31	53.98	Glycoprotein B
32	96.99	Phosphoprotein
33	64.78	Protease, capsid assembly protein
33.5	56.90	
34	46.65	Viral DNA cleavage/packaging
35	40.64	Membrane protein
36	36.82	Thymidine kinase
37	58.54	Glycoprotein H
38	46.40	Virion protein
39	50.35	Envelope protein, viral egress
40	45.56	Major capsid protein
41	75.52	Capsid protein
42.45	45.78	Spliced product, viral terminase
43	44.14	Viral DNA cleavage/packaging
44	58.44	Virion protein
46	47.85	Tegument protein
47	50.90	Protein kinase
48	57.03	DNase
49	72.63	Myristylated virion protein
50	79.49	Glycoprotein M
51	44.68	Origin binding protein
52	46.76	Component of DNA helicase-primase complex
53	49.52	γ-1 protein
54	39.64	Viral DNA cleavage/packaging
55	40.89	Component of DNA helicase-primase complex
56	44.86	γ-2 protein
57	69.38	Nonessential VZV protein
58	60.87	Phosphoprotein
59	52.41	Uracil DNA glycosylase
60	36.79	Glycoprotein L
61	57.71	Transcriptional activator, repressor, IE protein 1
62	36.02	Transcriptional activator, IE protein 3, duplicate of ORF 71
63	94.47	Transcriptional activator, IE protein 4, duplicate of ORF 70
64	57.29	Tegument phosphoprotein, duplicate of ORF 69
65	31.18	Tegument phosphoprotein
66	43.48	Protein kinase
67	53.52	Glycoprotein
68	74.80	Glycoprotein E

[a] IE, immediate early.

Data analysis. Desktop optical scanning was used to digitize each radiogram. Individual ORF intensities were quantitated with Quantity One densitometry software (Bio-Rad, Hercules, Calif.). Optical density (OD) for each SVV target was used to calculate the relative expression (RE) of each SVV ORF according to the following formula:

$$RE_i = OD_i/[(\overline{OD}_{no\ DNA})(\overline{OD}_{act})]$$

where RE_i is the relative expression of the ith SVV ORF, OD_i is the OD of the ith SVV ORF, $\overline{OD}_{no\ DNA}$ is the average OD for the no-DNA targets, and $\overline{OD}_{act}$ is the average OD for the actin targets. The denominator standardizes each radiogram for variations in background intensity or specific activity of the probe. To allow comparison of SVV transcription data with those published for VZV, the average relative SVV ORF expression (RE_i) obtained from all individual arrays was expressed as a percentage of the most abundant SVV ORF.

RESULTS

Macroarrays containing PCR fragments representing the entire SVV genome were constructed and probed with labeled SVV DNA or cDNA fragments. Figure 1 illustrates the specificity of the arrays examined with DNA probes as well as cDNA probes prepared from uninfected and SVV-infected cells. DNA probes from uninfected cells detected only actin (Fig. 1A), while DNA probes prepared from SVV-infected cells detected all 129 SVV DNA targets as well as actin (Fig. 1B). The signal intensities of actin after hybridization of DNA from both infected and uninfected cells were similar (Fig. 1A and B). cDNA probes from uninfected cells detected only actin (Fig. 1C), while cDNA probes from SVV-infected cells detected each of the 70 viral ORFs and actin (Fig. 1D). None of the probes hybridized to the negative controls (pGEM3zf$^-$ and no DNA). The signal intensities of actin after hybridization of cDNA from both infected and uninfected cells to actin were similar (Fig. 1C and D). Table 2 lists every ORF, region, location (row and column) on the array, relative expression of transcription, standard deviation for each SVV DNA target, and relative order of abundance 3 days after infection. For example, the 3′ end of ORF 9 is located in row 2 and column 7 on the array and is the most abundant transcript.

Figure 2 graphically displays the average spot intensity and standard deviation of each ORF in SVV-infected cells compared to those of a cellular transcript (actin). The values are the averages of three independent experiments in which the spot intensity for each SVV ORF was first divided by the product of the no-DNA and actin spot intensities and then normalized to the spot intensities obtained for the no-DNA and actin targets on three individual control arrays. All signal intensities of SVV ORFs are >1 standard deviation above the negative controls. Not unexpectedly, some variation in virus transcription was seen in the three samples of independently obtained RNA from SVV-infected cells (error bars in Fig. 2), but the relative expression of individual SVV genes was not affected (Table 2). Table 3 lists the average signal intensity of each SVV ORF 3 days after infection and their predicted gene function (4). The most abundant SVV transcript detected during productive infection is ORF 9 (tegument protein). Figure 3 graphically shows a comparison for the transcriptional abundance of each ORF for both SVV and VZV in cells 3 days after infection.

DISCUSSION

This study is the first to use macroarrays with chemiluminescence detection to study varicella virus gene expression during lytic infection in culture. Chemiluminescent probes are safer than radiolabeled probes for the investigator and the environment and can be stored for prolonged periods. Moreover, hybridization signals require shorter exposure times, and as little as 0.1 pg (700 genome equivalents) of labeled SVV DNA can be detected (data not shown). However, chemiluminescence applied to the study of cDNA can be capricious, and it often took multiple experiments to yield quantifiable results.

Digoxigenin-labeled DNA from SVV-infected cells hybridized to all array targets. Similarly, digoxigenin-labeled cDNA from SVV-infected cells hybridized to all array targets but with various signal intensities. Several factors, including the abundance of mRNA, RNA stability, and the efficiency of the reverse transcription reaction, may have influenced our observations. The longer or shorter half-life of SVV transcripts is probably compensated for by the decrease or increase in their abundance. A similar pattern of global transcription for the two varicella viruses was seen (Fig. 3). The four most abundant transcripts in SVV (i.e., ORFs 9, 32, 63, and 23) were found to be greater than the relative expression of actin. The levels of transcription for two of these (e.g., ORF 9 and 63) correlated well with that previously reported by array analysis for VZV (3). As in VZV, the most abundant ORF found in SVV during lytic infection was ORF 9. ORF 9 is predicted to encode a tegument protein. The herpes simplex virus type 1 homolog of varicella virus ORF 9, VP22 protein (herpes simplex virus type 1 UL49) has been shown to be one of the four proteins responsible for mediating capsid binding to the nuclear pore complex (7). Therefore, the ORF 9 protein in the tegument of SVV may be necessary for cell-to-cell infection. VZV ORF 63 is an immediate-early gene. SVV ORFs 32 and 23 were found to have a greater transcriptional abundance during the height of the cytopathic effect, while these ORFs in VZV were not as abundantly transcribed. VZV ORF 32 is predicted to encode a phosphoprotein and ORF 23 a capsid protein. Both of these VZV ORFs have less than 50% homology to SVV, which may explain the variations in transcriptional abundance. It is also possible that the stability of the mRNA transcribed from these VZV ORFs may be more stable than their SVV homologs. The SVV ORFs 62 to 64 and 69 to 71 map within the inverted repeat segment of the virus genome. By design, the array targets cannot differentiate between transcripts originating from either of the diploid genes. Therefore, ORF 62 to 64 expression levels determined by array analysis may be overrepresented by twofold (the difference attributed to ORF 69 to 71 transcription, respectively). The implication is that the promoter activity for these three diploid SVV genes may be lower than shown on Table 2. However, this report describes the steady-state levels of all SVV genes transcribed and not the specific promoter activities.

Overall, transcription from every SVV ORF could be identified in lytically infected cells using array technology and chemiluminescence detection.

ACKNOWLEDGMENTS

This work was supported in part by Public Health Service grants AG 06127 and NS 32623 from the National Institutes of Health. Steven Deitch is supported by Public Health Service grant NS 07321 from the National Institutes of Health.

We thank Marina Hoffman for editorial assistance and Cathy Allen for manuscript preparation.

REFERENCES

1. **Clarke, P., S. D. Rabkin, M. V. Inman, R. Mahalingam, R. Cohrs, M. Wellish, and D. H. Gilden.** 1992. Molecular analysis of simian varicella virus DNA. Virology **190:**597–605.
2. **Cohrs, R. J., J. Randall, J. Smith, D. H. Gilden, C. Dabrowski, H. van der Keyl, and R. Tal-Singer.** 2000. Analysis of individual human trigeminal ganglia for latent herpes simplex virus type 1 and varicella-zoster virus nucleic acids using real-time PCR. J. Virol. **74:**11464–11471.
3. **Cohrs, R. J., M. P. Hurley, and D. H. Gilden.** 2003. Array analysis of viral gene transcription during lytic infection of cells in tissue culture with varicella-zoster virus. J. Virol. **77:**11718–11732.
4. **Gray, W. L., B. Starnes, M. W. White, and R. Mahalingam.** 2001. The DNA sequence of the simian varicella virus genome. Virology **284:**123–130.
5. **Kennedy, P. G. E., E. Grinfeld, V. Traina-Dorge, D. H. Gilden, and R. Mahalingam.** 2004. Neuronal localization of simian varicella virus DNA in ganglia of naturally infected African green monkeys. Virus Genes **28:**273–276.
6. **Mahalingam, R., M. Wellish, W. Wolf, A. N. Dueland, R. Cohrs, A. Vafai, and D. Gilden.** 1990. Latent varicella zoster viral DNA in human trigeminal and thoracic ganglia. N. Engl. J. Med. **323:**627–631.
7. **Ojala, P. M., B. Sodeik, M. W. Ebersold, U. Kutay, and A. Helenius.** 2000. Herpes simplex virus type 1 entry into host cells: reconstitution of capsid binding and uncoating at the nuclear pore complex in vitro. Mol. Cell. Biol. **20:**4922–4931.